Oxygen transport and nonstoichiometry in SrFeO$_{3-\delta}$

Stefan DIETHELM[*], Alexandre CLOSSET, Jan VAN HERLE and Kemal NISANCIOGLU[a]

Laboratoire de Photonique et Interfaces, École Polytechnique Fédérale de Lausanne

CH-1015 Ecublens, Switzerland

a) Department of Materials Technology and Electrochemistry,

Norwegian University of Science and Technology,

N-7491 Trondheim, Norway

Abstract

Chemical diffusion ($\tilde{D}$) and surface exchange (k) coefficients for SrFeO$_{3-\delta}$ were measured using an electrochemical cell combined with electrochemical impedance spectroscopy (EIS) and potential step technique (PS) in the temperature range of 850-915°C. A $\tilde{D}$ value of ~ $4 \cdot 10^{-5}$ cm^2/s and a k value of ~ $8 \cdot 10^{-5}$ cm/s were obtained at 900°C. Slow scan (0.5-3 µV/s) cyclic voltametry (CV) was performed in the same temperature range, using the same electrochemical cell to obtain oxygen nonstoichiometry data. The oxygen nonstoichiometry (δ) at 900°C in air was determined as 0.4. A plateau corresponding to δ = 0.5 was observed below an oxygen partial pressure (pO_2) of 10^{-6} atm. These results were shown to be consistent with the literature data. Nonstoichiometry data were further analysed using the existing defect models, and the limits of the independent point defect approximation and the necessity of considering interactions between point defects and clusters were established.

Keywords: Strontium Ferrate/Ferrite; Oxygen transport; Oxygen nonstoichiometry.

1 Introduction

Since Teraoka and co-workers [1] have shown that, among $La_{1-x}Sr_xCo_{1-y}Fe_yO_{3-\delta}$ type of materials, the members of the $SrCo_xFe_{1-x}O_{3-\delta}$ family have exceptionally high oxygen transport rates, the interest in these materials has been increasing. They are considered as possible candidates for high temperature solid state electrochemical devices, in particular as dense oxygen separation membranes for partial oxidation of methane to syngas[2].

Besides oxygen transport properties, the structure of these materials, in particular oxygen nonstoichiometry, has been extensively studied, especially for the end members $SrFeO_{3-\delta}$[3] and $SrCoO_{3-\delta}$[4]. It was shown, by high temperature gravimetry and high temperature powder X-ray diffraction (XRD) analysis under controlled oxygen partial pressure (pO_2), that, in the temperature range of 400-900°C, $SrFeO_{3-\delta}$ consists of the brownmillerite-type $SrFeO_{2.5}$ and the cubic perovskite-type $SrFeO_{3-\delta}$ with large oxygen deficient-type nonstoichiometry. Above 900°C, the brownmillerite phase transforms to the perovskite phase[5].

More recently, the phase diagram of $SrCo_{0.8}Fe_{0.2}O_{3-\delta}$ has been determined as a function of temperature and pO_2 by thermogravimetric analysis[6]. As for $SrFeO_{3-\delta}$, two phases with perovskite and brownmillerite structures were observed below 770°C. Above this temperature, only the perovskite type phase was stable. In that study the oxygen nonstoichiometry (δ) was shown to be as large as 0.57 (3-δ = 2.43) at 850°C and $pO_2 = 5 \cdot 10^{-4}$ atm.

The transition between the perovskite-type phase, where the oxygen vacancies are supposed to be randomly distributed, and the brownmillerite type phase, in which the oxygen vacancies are ordered[7], is known to affect dramatically the oxygen transport properties of such materials[8]. However, defect models describing highly nonstoichiometric materials are

still lacking, and, therefore, the influence of large nonstoichiometry on the transport properties needs further investigation. In this respect, the members of the $SrCo_xFe_{1-x}O_{3-\delta}$ series are of particular interest.

In previous work, oxygen transport in $SrCo_{0.5}Fe_{0.5}O_{3-\delta}$ was characterised using a specially designed electrochemical cell[9] together with electrochemical impedance spectroscopy (EIS)[10] and potential step (PS)[11] techniques. Oxygen chemical diffusion and surface exchange coefficients could be obtained from a single shot experiment. Furthermore, the electrochemical cell functioned as a coulometric titration cell from which additional information about the oxygen nonstoichiometry of the material could be obtained.

In this study, we have applied the same techniques to compound $SrFeO_{3-\delta}$ in order to obtain chemical diffusion and surface exchange coefficients in the temperature range of 850 – 915 °C. In addition, nonstoichiometry data were obtained by use of slow scan rate (0.5 –3 μV/s) cyclic voltametry[12] in the same temperature range and in the pO_2 range of $0.21 - 10^{-10}$ atm. These results are discussed in terms of existing defect models.

2 Experimental

SrFeO$_{3-\delta}$ powder was prepared using a spray pyrolysis technique with nitrate solutions of the metal ions, followed by ball milling and calcination at 900°C for 10 hours. The phase purity was checked by XRD analysis. Sample discs were obtained by double-action uniaxial pressing at 7 MPa followed by cold isostatic pressing (CIP) at 140 MPa. The pellets were then sintered at 930°C for 3 hours and slowly cooled in air.[13] A bulk density of the sintered disc of 4.92 g/cm^3, corresponding to a relative density of 91%, was measured by the Archimedean method.

The electrochemical cell design used in this study is shown in Fig. 1. It consisted of a dense specimen pellet blocked ionically on one surface by a platinum foil. The opposite surface was left bare. An annular gold spacer separated the surface from a YSZ slab coated on both sides with porous platinum. The latter was used as an oxygen pump enabling control of the oxygen partial pressure within the gas space between the specimen and YSZ slab[11]. $SrFeO_{3-\delta}$[14] and $SrCo_{0.5}Fe_{0.5}O_{3-\delta}$[15] being good electronic conductors, the upper porous Pt layer was connected to the current feeder across the specimen pellet. The cylindrical surface of the specimen was sealed with glass. The cell was clamped between two alumina tubes at the centre of a cylindrical furnace.

All electrochemical measurements were performed using an EG&G (PAR 273) potentiostat computer controlled by Corrware software. For EIS measurements, an EG&G (1025) frequency response analyser, run by M398 software, was used.

3 Theory

3.1 Oxygen transport

The theoretical model describing the transport of oxygen in mixed conducting oxides has been discussed in detail elsewhere[16] on the basis of C. Wagner's work[17] and will thus not be repeated here. In this section, we will only present the expressions which are used in the analysis of the experimental data for both PS and EIS experiments. Basically, these expressions are derived from Fick's phenomenological law for chemical diffusion with first order kinetics assigned to the gas-solid interface reaction.

For the relaxation current resulting from a potential-step, i.e. a step-wise modification of the oxygen activity at the gas-solid interface, the asymptotic expressions valid respectively for short and large times are [11]

$$I(t) = \frac{Q\,k}{L}\left(1 - 2k\sqrt{\frac{t}{\pi\,\tilde{D}}}\right) + \mathbf{O}(t) \qquad\qquad t << \tilde{D}/k^2 \qquad\qquad [1]$$

and

$$I(t) = \frac{2Qk^2}{\tilde{D}(\lambda_1^2 + \Lambda^2 + \Lambda)}\exp\left(\frac{-\lambda_1^2\,\tilde{D}t}{L^2}\right) \qquad\qquad t >> L^2/\tilde{D}\pi^2 \qquad\qquad [2]$$

where Q is the total charge passed as t tends to infinity, L is the thickness of the sample and λ_1 is the first positive root of

$$\lambda_n \tan \lambda_n = \Lambda \qquad\qquad\qquad \text{and} \quad \Lambda = kL/\tilde{D}\;.$$

Similarly, the complex impedance corresponding to the diffusion problem has been derived[10]

$$Z_{diff}(j\omega) = \frac{dE}{d\delta}\frac{V_m}{2FS}\left(\frac{1}{k} + \frac{1}{\sqrt{j\omega\,\tilde{D}}}\coth L\sqrt{\frac{j\omega}{\tilde{D}}}\right) = R_s + Z_W(\omega) \qquad\qquad [3]$$

where F is Faraday's constant, V_m is the molar volume of the sample, S is the area of the oxygen exchange surface and $(dE/d\delta)$ is the slope of the coulometric titration curve. Expression [3] consists of the sum of a purely resistive (R_s) term which describes the surface exchange reaction and the well known finite length diffusion element (Z_W).

3.2 Coulometric titration

The electrochemical cell displayed in Figure 1 can be used to control the oxygen nonstoichiometry (δ) of the oxide sample. In the case of a potential step experiment, the change in the oxygen nonstoichiometry ($\Delta\delta$) is directly obtained by integrating the relaxation current between the initial and final equilibrium state,

$$\Delta\delta = \frac{\Delta Q\,M}{2Fm} \qquad\qquad [4]$$

where ΔQ is the total charge extracted from the sample during the potential step, M is the molecular weight of the sample, m is its weight, and F is Faraday's constant. For a sufficiently small potential step, the slope of the coulometric titration curve $dE/d\delta$ can thus be expressed as

$$\frac{dE}{d\delta} \cong \frac{\Delta E}{\Delta \delta} = \frac{2Fm\Delta E}{\Delta Q\, M} \tag{5}.$$

In a similar way, $dE/d\delta$ can be obtained from the capacitive behaviour of the impedance data at very low frequencies.[10]

In the case of cyclic voltametry, equilibrium is never reached since the applied voltage is continuously varied. Titration is thus only possible if the sweep rate is sufficiently slow in order to remain close to equilibrium. This condition will be discussed further in section 4.2.

The reversible potential difference across the oxygen pump, which is needed to evaluate the pO_2 in the gas space, can be estimated from the applied potential by correcting for the ohmic drop in the electrolyte and the polarisation overpotential of the Pt electrodes in the presence of a current,

$$\Delta E = \Delta V - R_e i - \eta(i) \tag{6}$$

where R_e is the resistance of the electrolyte, and η the polarisation overpotential of the Pt electrodes. Both corrections can be estimated by EIS. It is assumed that, for the current range measured in the experiments (i < 1 mA), $\eta(i)$ can be linearised,

$$\Delta E = \Delta V - (R_e + R_1)\, i \tag{7}$$

where R_1 stands for the polarisation resistance of the Pt electrodes. Following the development of Jacobsen and co-workers,[12] we can write the current of the cell in terms of three contributions

$$i = i_S + i_G + i_L \qquad [8]$$

where i_S is the current due to the oxygen leaving the sample, i_G is the supply of oxygen necessary to adjust the pO_2 in the gas space between the oxygen pump and the sample, and i_L is the sum of the currents due to gas leakage through the glass seal and electronic current through the electrolyte. In the case of the electrochemical cell used in this study, i_G is negligible and will not be considered further. The leakage current i_L should be small compared to the current drawn from the sample. We assume that it is proportional to the pO_2 difference between the gas space and the surrounding air and thus, using Nernst's law,

$$i_L = \alpha \, (1 - \exp(- 4F\Delta E/\Re T)) \qquad [9]$$

where $\Re$ is the ideal gas constant, and α is a proportionality factor which can be determined from the steady state current at high potentials as discussed later in section 4.2.

The slope of the coulometric titration curve can be expressed in the form

$$\frac{dE}{d\delta} = \frac{2Fm}{M}\frac{dE}{dQ} = \frac{2Fm}{M}\frac{dE}{dt}\frac{dt}{dQ} = \frac{2Fm}{M}\frac{dE}{dt}(i_S)^{-1} \qquad [10]$$

The change in nonstoichiometry for a given potential difference ΔE is obtained by integration of [10],

$$\delta(\Delta E) = \int\limits_{E_0}^{E_0 + \Delta E} \frac{M}{2Fm}\left[\frac{dE}{dt}\right]^{-1} i_S(E)\, dE \qquad [11]$$

3.3 Defect models

In this section three existing defect models will briefly be reviewed. In all models, the oxygen vacancies are assumed to be fully ionised and are the only ionic defects present in $SrFeO_{3-\delta}$. It is further assumed that the only electronic defects present in the pO_2 range $0.21 - 10^{-10}$ atm are Fe^{3+} ions.[3]

The oxygen exchange reaction can then be written as, in the Kröger-Vink notation,[18]

$$\tfrac{1}{2}\, O_2{}^{gas} + V_O{}^{\bullet\bullet} + 2\, Fe_{Fe}{}' \;\surd\; O_O{}^{x} + 2\, Fe_{Fe}{}^{x} \qquad [12]$$
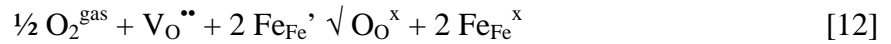
By assuming independent (noninteracting) point defects, it is possible to write a mass-action-relation of type

$$pO_2{}^{\frac{1}{2}}\, [V_O{}^{\bullet\bullet}]\, [Fe_{Fe}{}']^2 = K\, [O_O{}^{x}]\, [Fe_{Fe}{}^{x}]^2 \qquad [13]$$

where [ ] is the bulk concentration expressed in mol/cm^3, and K is the equilibrium constant. The site conservation condition for iron and oxygen and the condition of local electroneutrality give the three additional relations

$$[Fe_{Fe}{}^{x}] + [Fe_{Fe}{}'] = \rho/M \qquad [14]$$

$$[O_O^x] + [V_O^{\bullet\bullet}] = 3\rho/M \qquad [15]$$

$$2[V_O^{\bullet\bullet}] = [Fe_{Fe}'] \qquad [16]$$

where ρ is the density of the sample, and M is its molecular weight. Substituting relations [14]-[16] into [13] and using the relation between the oxygen nonstoichiometry δ and the oxygen vacancy concentration $[V_O^{\bullet\bullet}]$, $[V_O^{\bullet\bullet}] = \delta\rho/M$, one obtains

$$pO_2 = K^2 \frac{(1-2\delta)^4 (3-\delta)^2}{16\delta^6} \qquad [17]$$

This expression assumes that the point defects are independent, which restricts its validity to small defect concentrations, and thus, it should not apply to our case.

A way of taking into account possible interactions between the point defects is to restrain this interaction to neighbouring sites by assuming that clusters are formed by strong attractive interaction. This model was proposed by van Roosmalen and Cordfunke[19] and successfully applied to $LaMnO_{3-\delta}$ and $LaCoO_{3-\delta}$. In this case, the oxygen incorporation reaction becomes

$$\text{½ } O_2^{gas} + <Fe_{Fe}'\text{-}V_O^{\bullet\bullet}\text{-}Fe_{Fe}'>_C \; \surd \; O_O^x + 2\,Fe_{Fe}^x \qquad [18]$$
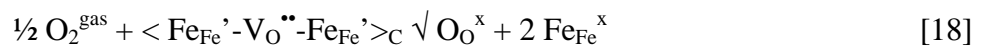
where $<Fe_{Fe}'\text{-}V_O^{\bullet\bullet}\text{-}Fe_{Fe}'>_C$ is a cluster in which an oxygen vacancy is associated with two Fe^{3+} ions. The restriction of the interaction to neighbouring sites enables us to treat the clusters as independent defects and thus write the equation

$$pO_2^{½}[<Fe_{Fe}'\text{-}V_O^{\bullet\bullet}\text{-} Fe_{Fe}'>_C] = K_C\,[O_O^x]\,[Fe_{Fe}^x]^2 \qquad [19]$$

and further by using the site conservation conditions,

9

$$pO_2 = K_C{}^2 \ \frac{(1-2\delta)^4(3-\delta)^2}{\delta^2} \qquad [20]$$

This model will be referred to as the cluster model.

An alternative description of short range interaction was proposed by Ling.[20] It is based on a statistical thermodynamic approach which assumes that each defect cluster reduces by a factor Λ the number of available ways of placing an additional defect. It is thus called the generalised exclusion concept. This leads to the relationship[21]

$$pO_2 = K_{EC} \ \frac{(3-\Lambda\,\delta)^2}{\delta^2} \qquad [21]$$

This model will be referred to as the excluded configuration model.

Further details about the derivation of these models can be found in a review article by Lankhorst and co-workers. [21]

4 Results

4.1 Oxygen transport measurements

Chemical diffusion coefficients of $SrFeO_{3-\delta}$ were obtained by analysing the current relaxation resulting from potential steps, using the asymptotic expressions [1] and [2] as described elsewhere in detail.[11] In addition, EIS measurements were performed on the same cell. The resulting impedance data could either be analysed in the complex plane by using an equivalent circuit or using asymptotic expressions in Bode-type plots.[10] The equivalent circuit used in this study (cf. Figure 2) was derived from mass balance considerations and applied with success to $SrCo_{0.5}Fe_{0.5}O_{3-\delta}$.[10] The first element, R_e, corresponds to the ohmic

drop in the electrolyte as measured by the reference electrode. The second element, which consists of a constant phase element (CPE$_1$) in parallel with a resistance, R$_1$, describes the impedance of the platinum electrodes[22]. The last element corresponds to the diffusion impedance described by equation [3], where Z$_W$ stands for the finite length diffusion, and the resistive element R$_s$ takes into account the surface exchange limitation. The additional CPE$_2$ set in parallel, describes the contribution of the gaseous oxygen in the gas space and adsorbed oxygen.[10] As an illustration, Figure 2 shows the impedance response to a 5 mV amplitude modulation in the frequency range of 100 kHz to 50 µHz with a dc bias of –20 mV at 900°C, along with its fit to the equivalent circuit discussed above.

The chemical diffusion coefficients ($\tilde{D}$) obtained from the two methods at different temperatures are reported in an Arrhenius plot (Figure 3). Data for SrCo$_{0.5}$Fe$_{0.5}$O$_{3-\delta}$ obtained in a previous study are also presented for comparison. The error bars assigned to the values obtained by EIS have been calculated from the difference between experimental data and fitted data according to the equivalent circuit model. They cover the discrepancy between the EIS and PS data in the case of SrCo$_{0.5}$Fe$_{0.5}$O$_{3-\delta}$ but not of SrFeO$_{3-\delta}$, especially above 900°C. The apparent scatter for SrFeO$_{3-\delta}$ should be regarded as relevant of the quality of the data, with 20% error at 900°C. Despite this scatter, the chemical diffusion coefficients are a factor 2-3 higher for SrFeO$_{3-\delta}$.

Although no linear behaviour can be ascertained in this temperature range due to the scatter, an average activation energy close to 200 kJ/mol was estimated for both materials.

The surface exchange coefficients (k) were evaluated from the R$_S$ values obtained by fitting the equivalent circuit to the impedance data, using equation [3].[10] They are shown in an Arrhenius plot (Figure 4) with the corresponding data for SrCo$_{0.5}$Fe$_{0.5}$O$_{3-\delta}$. In this case, the tendency is reversed; the rate at which oxygen is exchanged at the oxide surface is enhanced in the case of SrCo$_{0.5}$Fe$_{0.5}$O$_{3-\delta.}$

4.2 Oxygen nonstoichiometry

A complete slow scan (3 µV/s) cyclic voltammogram is shown in Figure 5. As the voltage is decreased, the current tends to a steady state value. This value was taken as the leakage current and used as the proportionality factor α in Equation [9]. This approach is different from that proposed by Jacobsen and co-workers,[12] but leads in the present case to oxygen nonstoichiometric data which are in better agreement with the literature data.

As mentioned previously, the condition of being "close to equilibrium" is crucial for the validity of the present approach. This condition is satisfied if the change in nonstoichiometry is independent of the scan rate. According to equation [11], this would require that the integrand $((dt/dE)i_S)$ is independent of the scan rate. Figure 6 shows the current corresponding to two different scan rates, 3 µV/s and 0.5 µV/s, differing by a factor of 6. By multiplying the slow scan current by this factor the high scan values were reproduced within 10-15% error, as indicated in the figure. Considering that the current response to the slowest scan rate is very noisy, the agreement is acceptable.

However, this verification was not used systematically because it is too time-consuming. An alternative approach is to compare the $dE/d\delta$ value obtained from slow scan CV with the corresponding values obtained at equilibrium from EIS and potential step measurements. Table 1 gives $dE/d\delta$ values obtained from the three methods at different temperatures. At 900°C, the agreement is excellent for both of the bias potentials -20 and –40 mV. At 915°C, the comparison is difficult because of certain differences in the experimental conditions. However, the tendency of decreasing $dE/d\delta$ with decreasing potential is obeyed. Furthermore, as the transport rate is enhanced with increasing temperature, the good agreement at 900°C

implies that the equilibrium assumption should be satisfied for all temperatures above 900°C. Agreement is not as good below 900°C. Since the activation energy for diffusion is large, the rate of oxygen transport decreases dramatically with decreasing temperature and exceptionally slow scan rates are required to satisfy the equilibrium assumption. This is the major drawback of using pellet instead of powder specimen.

The oxygen nonstoichiometry data was obtained from equation [11], after correcting i_S for leakage in the manner described. This gives the relative change of nonstoichiometry $\Delta\delta$ as a function of the potential vs. air. As ΔE refers to equilibrium, the corresponding pO_2 was calculated from Nernst's law. In evaluating the absolute oxygen nonstoichiometry δ, the asymptotic plateau obtained in the data with decreasing pO_2 was normalised at $\delta = 0.50$ following the approach of Mizusaki and co-workers.[5] At the plateau, Fe^{4+} is completely reduced to Fe^{3+} which can further be reduced to Fe^{2+} but at much lower pO_2. Figure 7 shows the so obtained nonstoichiometry data at 900 and 915°C. For comparison, the data obtained by Mizusaki and co-workers[5] from high temperature gravimetry at 900°C is presented in the same figure. The present results show satisfactory agreement with the literature data.

4.3 Fit to defect models

The nonstoichiometry data were fitted to equations [17], [20] and [21] by a non-linear least square fit analysis. The exclusion factor in [21] was fixed at 6 in order to reproduce the plateau at $\delta = 0.5$. The unknown equilibrium constants were obtained from the regression analysis, and the resulting values are reported in table 2. Figures 8 and 9 show the best fits of the nonstoichiometry data at 900 and 915°C, respectively, to the three defect models. As seen

from the figures, none of these models gives a good fit to data over the entire pO_2 range of interest. However, no attempts were made to improve the models, and thus, this part of the study should be considered as preliminary.

5 Discussion

The chemical diffusion coefficients obtained for $SrFeO_{3-\delta}$ are very high, as expected from other published data.[1],[23] However, the fact that they are higher than for $SrCo_{0.5}Fe_{0.5}O_{3-\delta}$ is unexpected in view of the data of Teraoka and co-workers [1] which showed that the oxygen permeation rate through the $SrCo_xFe_{1-x}O_{3-\delta}$ series of compounds increased with increasing content of Co, which gave an increase in the oxygen nonstoichiometry.[24] According to the independent point defect theory, the chemical diffusion coefficient should increase with the oxygen vacancy concentration. Given the large oxygen deficiency of these materials (14 and 16 % in air at 900°C for $SrFeO_{3-\delta}$[5] and $SrCo_{0.8}Fe_{0.2}O_{3-\delta}$[6] respectively), however, interactions between the defects have to be considered to understand lower than expected mobility of oxygen in these materials. Furthermore, the critical thickness, $L_C = \tilde{D}/k$,[25] below which the permeation flux becomes governed by the rate of surface exchange reaction is large for such materials, typically 1.2 mm for $SrCo_{0.5}Fe_{0.5}O_{3-\delta}$ at 850°C and 12 mm for $SrFeO_{3-\delta}$ at 875°C, according to this study's results. Thus, the permeation flux measured by Teraoka and co-workers may have been governed by the surface exchange rate, which would explain the higher fluxes for $SrCo_{0.5}Fe_{0.5}O_{3-\delta}$, since this compound has higher k values than $SrFeO_{3-\delta}$ (cf. Figure 4).

14

It is clear from Figure 8 that the cluster model gives the best fit to data at high pO_2, in the range of 0.3 to 10^{-2} atm, and at low pO_2, the best fit is given by the excluded configurations model. As expected, the independent defect model does not give a correct description of highly defective oxides. Furthermore, the good agreement at high pO_2 obtained with the cluster model can be interpreted as a possible association of neighbouring defects of opposite relative charges to form neutral clusters ($<Fe_{Fe}'-V_O^{\bullet\bullet}-Fe_{Fe}'>_C$) through electrostatic attraction. As pO_2 is reduced, i.e., the concentration of defects is increased, the approximation of independent clusters seems to fail. An improved model has to take into account interactions between clusters. This is roughly done by the excluded configurations model, but the assumption that the number of excluded configurations per cluster (Λ) is independent of the number of existing clusters is probably unrealistic.

In the light of these considerations, the exceptionally high activation energies of the chemical diffusion coefficients can contain an additional contribution due to the interaction energy between defects. This would be similar to the trapping effect discussed by Maier.[26] Furthermore, a slight bending, which is apparent at high temperature in figure 3, especially for $SrCo_{0.5}Fe_{0.5}O_{3-\delta}$, corresponds to a decrease of the activation energy. As the temperature is increased, the vibrational energy of the lattice increases and counteracts the cohesive interaction between the defects, thereby lowering the energy necessary to displace the defects.

At this point the discussion regarding the structure of these materials is at best speculative considering the assumptions underlying the models used in this study, and further work is in progress.

6 Conclusions

Chemical diffusion and surface exchange coefficients of compound $SrFeO_{3-\delta}$ were measured by EIS and the potential step technique. A $\tilde{D}$ value of $\sim 4 \cdot 10^{-5}$ cm^2/s at 900°C was obtained, which is a factor of 2-3 higher than the value for $SrCo_{0.5}Fe_{0.5}O_{3-\delta}$. The k values of $SrFeO_{3-\delta}$ were however smaller than for $SrCo_{0.5}Fe_{0.5}O_{3-\delta}$, by a factor 3.

It was further shown that, by applying slow scan cyclic voltammetry to the same electrochemical cell, reliable oxygen nonstoichiometry data could be obtained. Analysis of the nonstoichiometry data by using existing defect models showed the limits of the independent point defect approximation and the necessity of considering interactions between point defects and clusters. No conclusions could be obtained about the defect chemistry of these highly defective perovskite type materials. However, a basis was provided for further work.

T/°C	SSCV	EIS	PS
915	-1.79 (-30mV)	-1.48 (-20mV)	-1.47 (0 → -20mV)
900	-1.34 (-20mV) -1.49 (-40mV)	-1.36 (-20mV) -1.50 (-40mV)	-1.29 (0 → -20mV) -1.62 (-24 → -40mV)
875	-1.45 (-20mV)	-1.32 (-20mV)	-1.23 (0 → -20mV)
850	-1.34 (-20mV)	-	-1.12 (0 → -20mV)

Table 1. Values of dE/dδ at different temperatures expressed in V and obtained from slow scan cyclic voltammetry (SSCV), electrochemical impedance spectroscopy (EIS) and potential step (PS). The corresponding cell potential (dc bias) is expressed in parenthesis.

T/°C	Point defect	Cluster	Excluded configurations
915	$K^2 = 8.296 \pm 0.028$	$K_C^2 = 12.82 \pm 0.03$	$K_{EC} = 0.085 \pm 0.001$
900	$K^2 = 1.169 \pm 0.003$	$K_C^2 = 2.924 \pm 0.003$	$K_{EC} = 0.0803 \pm 0.0008$

Table 2. Equilibrium constants calculated from equations [17], [20] and [21] by regression analysis of experimental nonstoichiometry data.

Figure captions

Figure 1: Cell design used for all electrochemical measurements.

Figure 2: Impedance response to a 5 mV amplitude modulation in the frequency range of 100 kHz to 50 µHz with a dc bias of –20 mV vs. air at 900°C. The best fit to the equivalent circuit is also displayed. Refer to text for an explanation of the equivalent circuit elements.

Figure 3: Arrhenius plot for chemical diffusion coefficients of $SrFeO_{3-\delta}$ and $SrCo_{0.5}Fe_{0.5}O_{3-\delta}$ samples, calculated from current transients following potential steps of –20 mV vs. air (PS) and from impedance data (EIS).

Figure 4: Arrhenius plot for surface exchange coefficients of $SrFeO_{3-\delta}$ and $SrCo_{0.5}Fe_{0.5}O_{3-\delta}$ samples, obtained by fitting the impedance data to the equivalent circuit in Figure 2.

Figure 5: Cyclic voltammogram for $SrFeO_{3-\delta}$ at 915°C, obtained at a scan rate of 3 µV/s.

Figure 6: Current vs. potential curves corresponding to two different scan rates at 900°C. Open circles (O) represent the current calculated by multiplying the 0.5 µV/s data by the scan rate ratio of 6.

Figure 7: Nonstoichiometry data (δ) vs. pO_2 for $SrFeO_{3-\delta}$ at 900 and 915°C, obtained by integrating the current drawn from the sample according to Equation [11]. The data of Mizusaki and co-workers [5] obtained at 900°C are also shown for comparison.

Figure 8: Best fits of the oxygen nonstoichiometry data δ of $SrFeO_{3-\delta}$ at 900°C to the point defect model (Equation [17]), the cluster model (Equation [20]) and the excluded configurations model (Equation [21]).

Figure 9: Best fits of the oxygen nonstoichiometry data δ of $SrFeO_{3-\delta}$ at 915°C to the point defect model (Equation [17]), the cluster model (Equation [20]) and the excluded configuration model (Equation [21]).
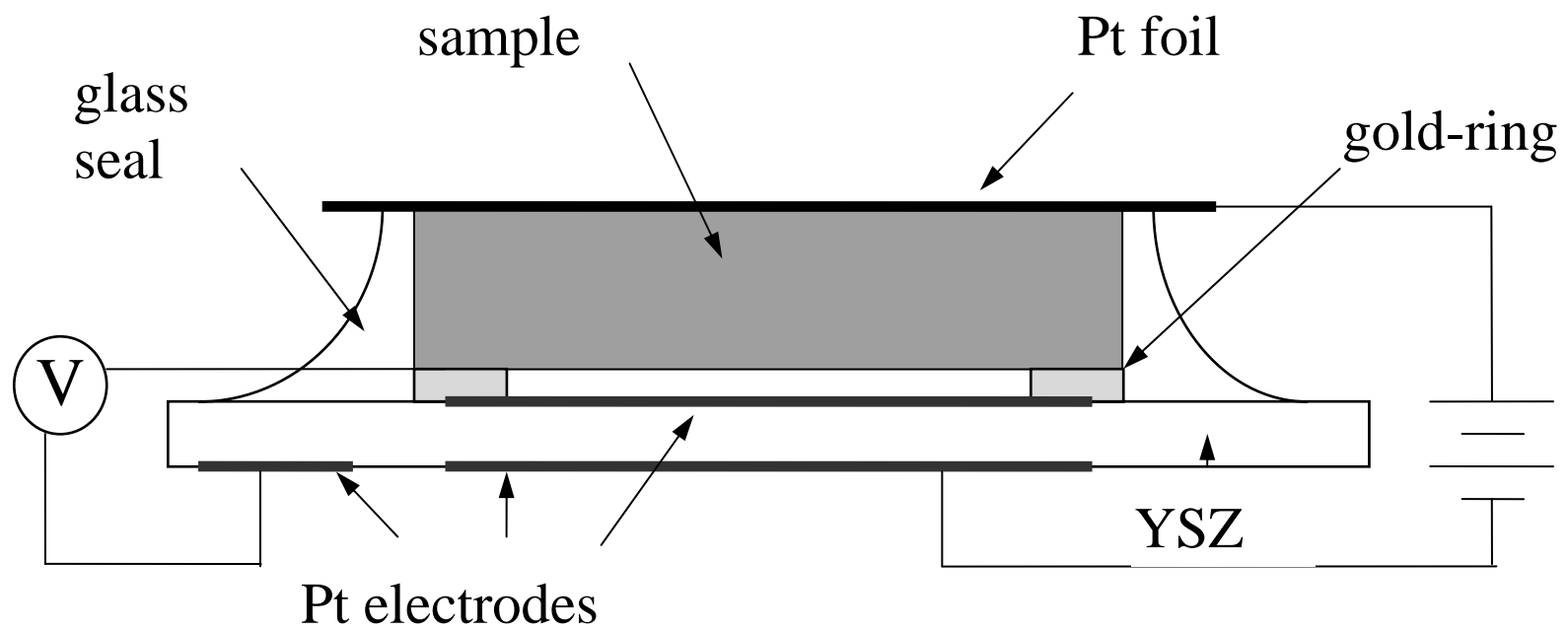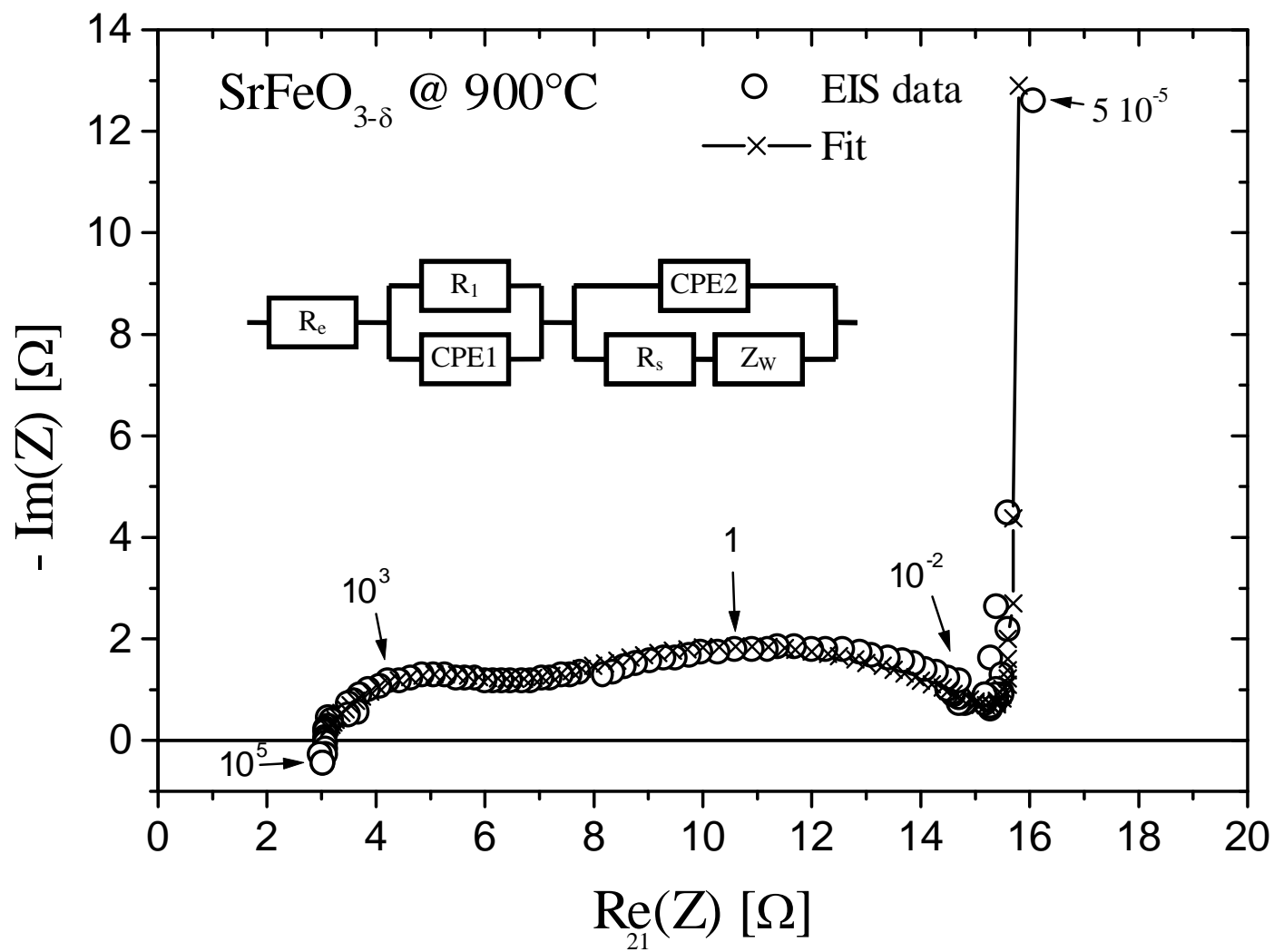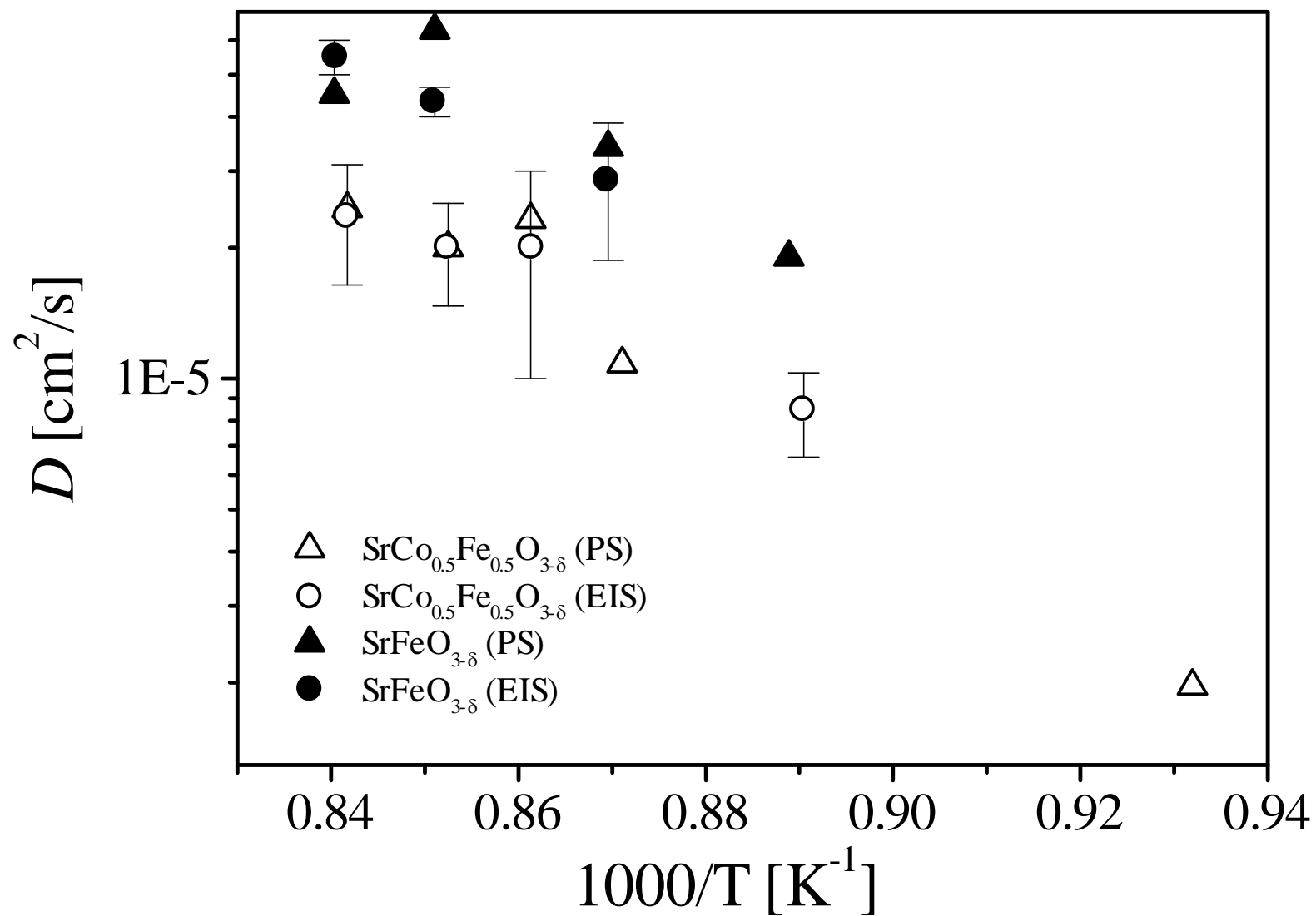
Figure 1

glass
seal

sample

Pt foil

gold-ring

V

Pt electrodes
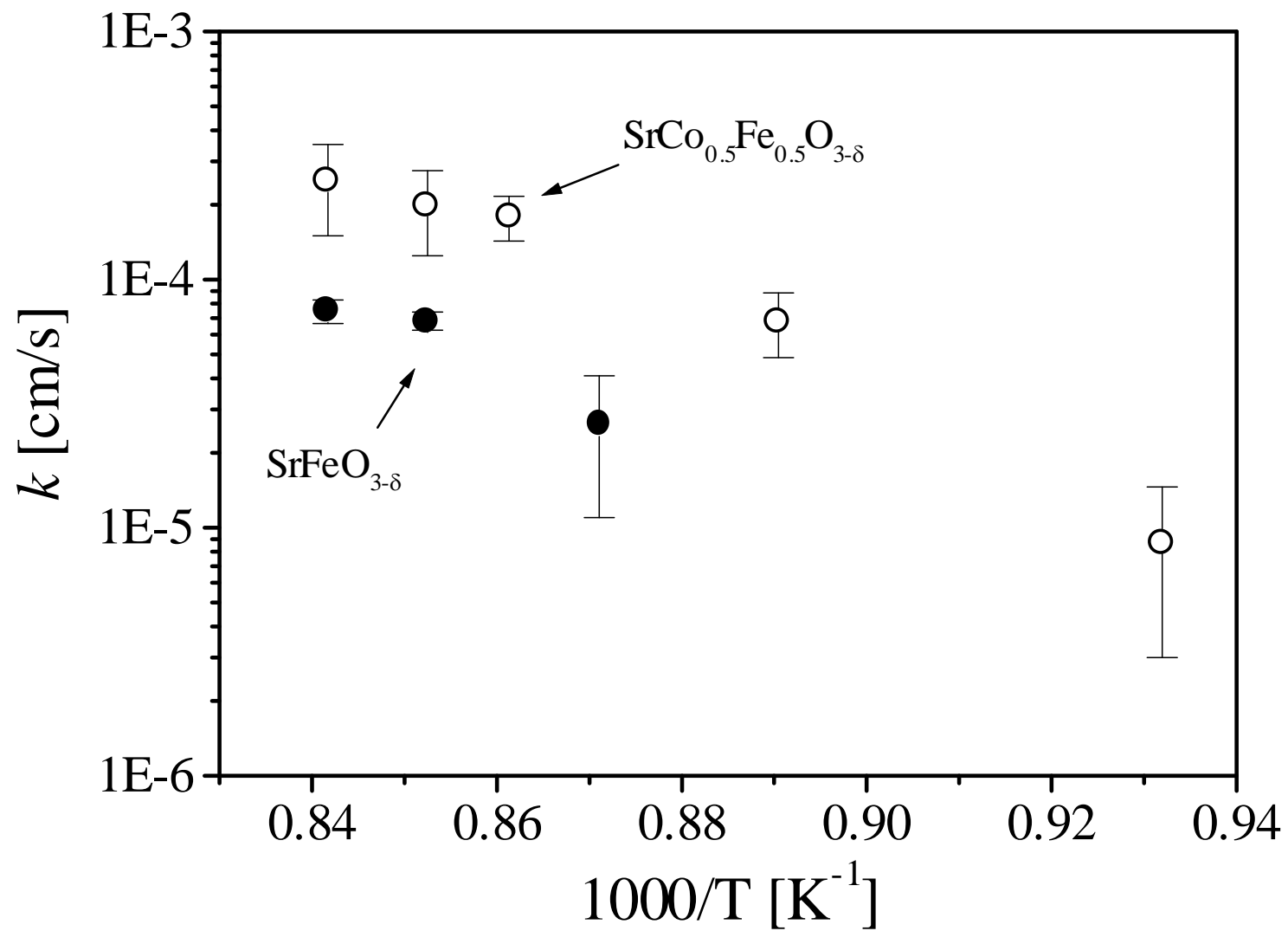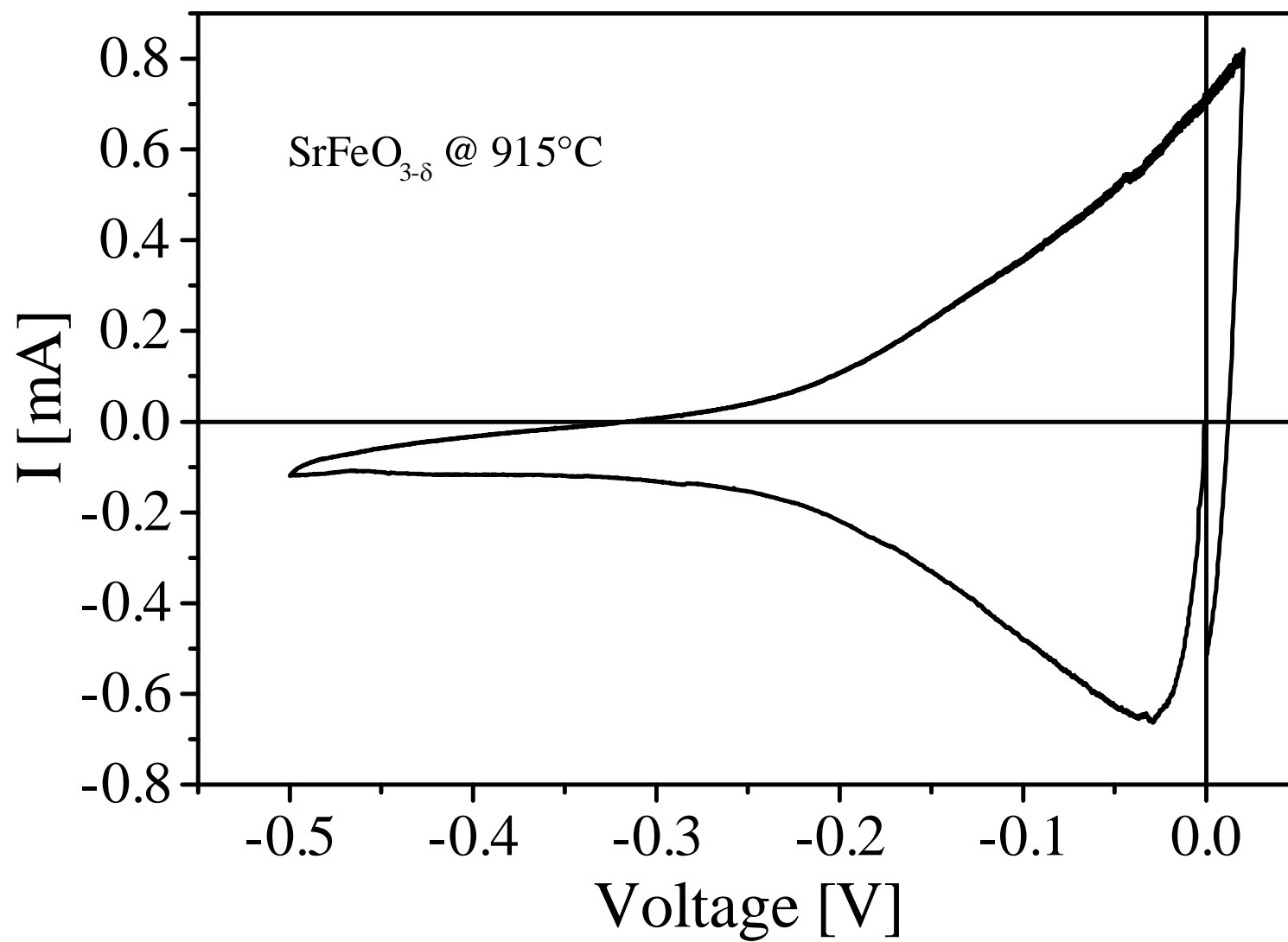
YSZ

Figure 2

Figure 3

Figure 4

Figure 5

SrFeO$_{3-\delta}$ @ 915°C

Figure 6

Figure 7

Figure 8

Figure 8. $SrFeO_{3-\delta}$ @ 900°C with curves for excluded configurations, cluster model, and point defect model. Axes: δ versus pO_2 [atm.].
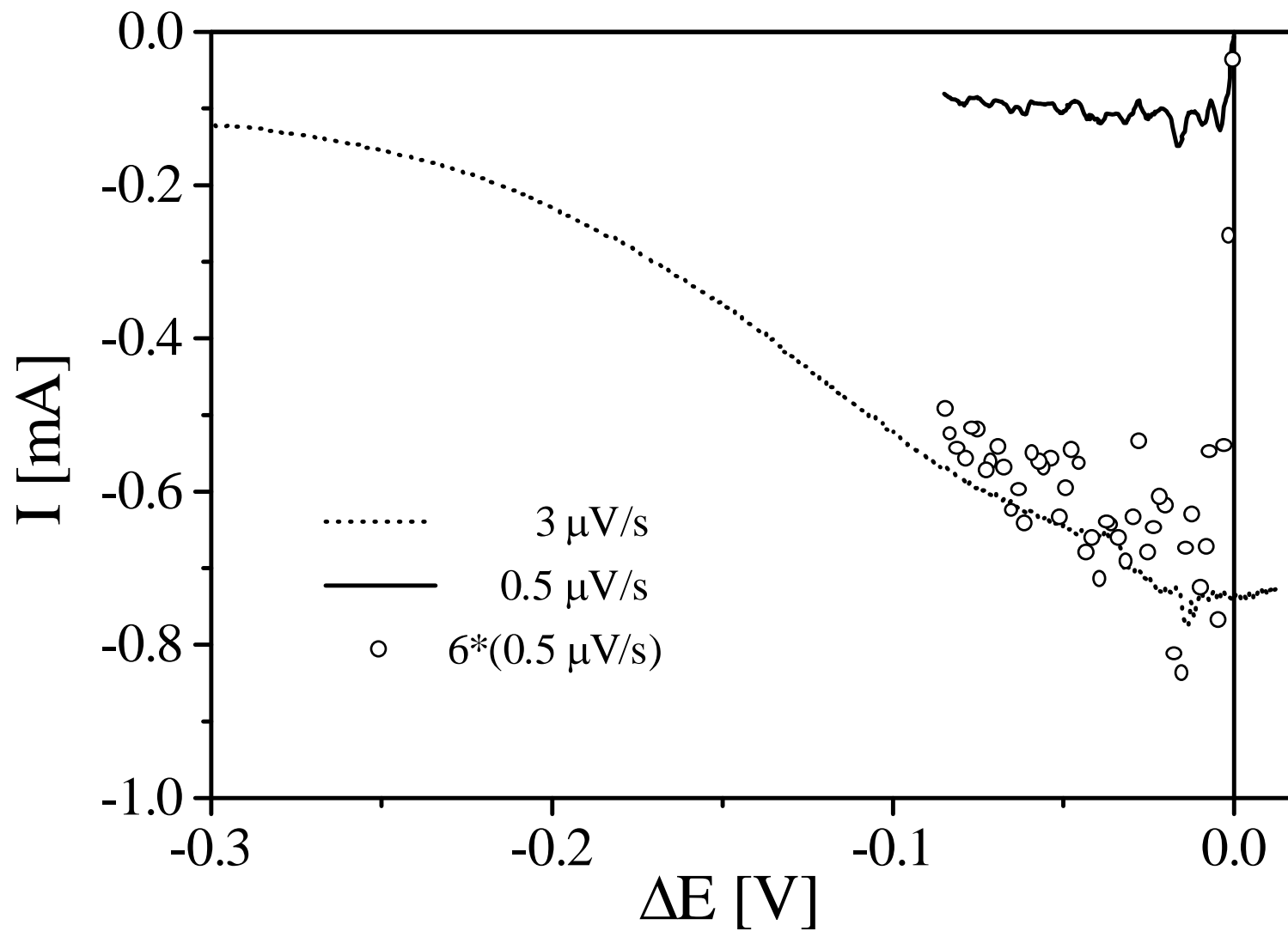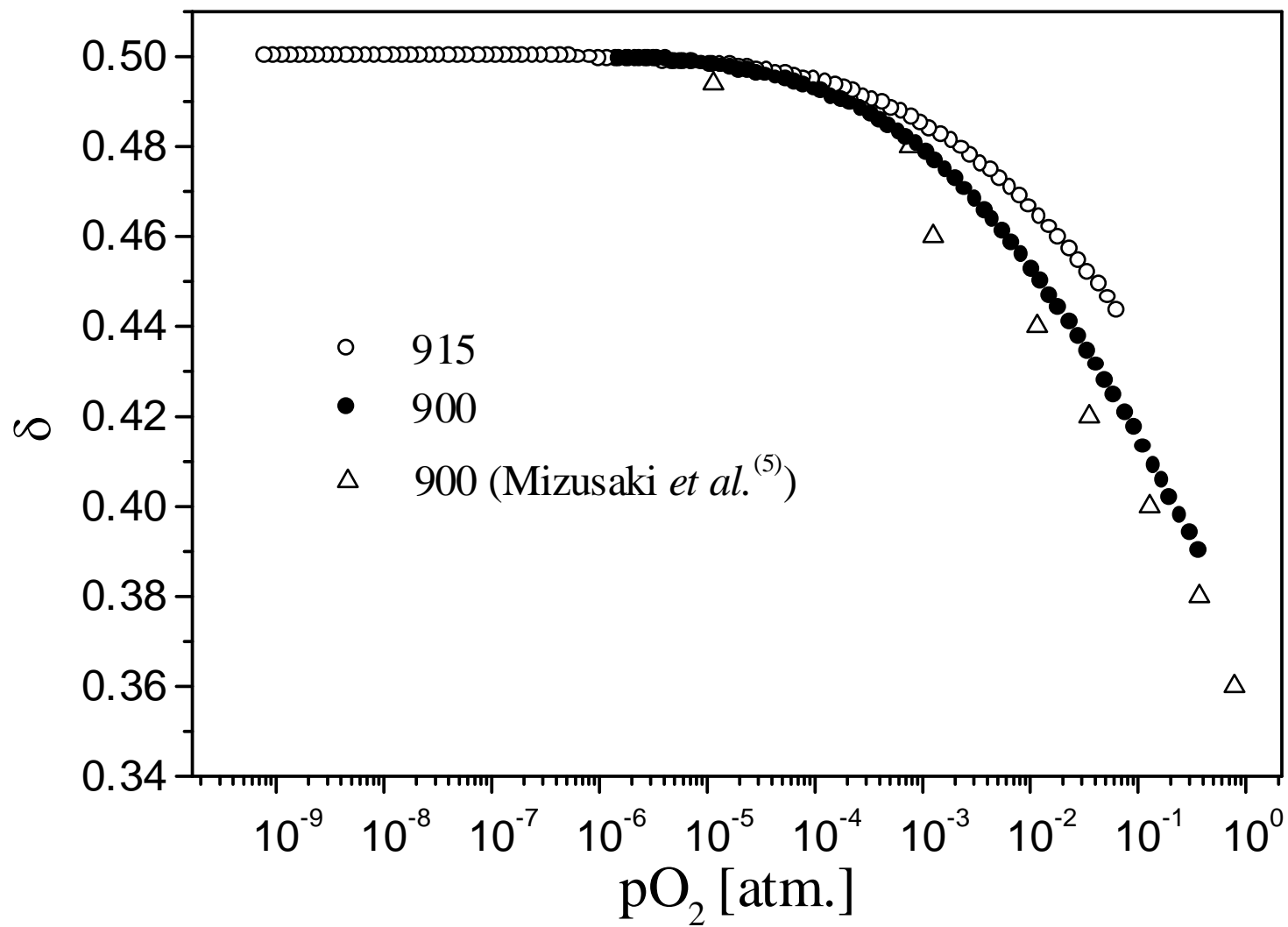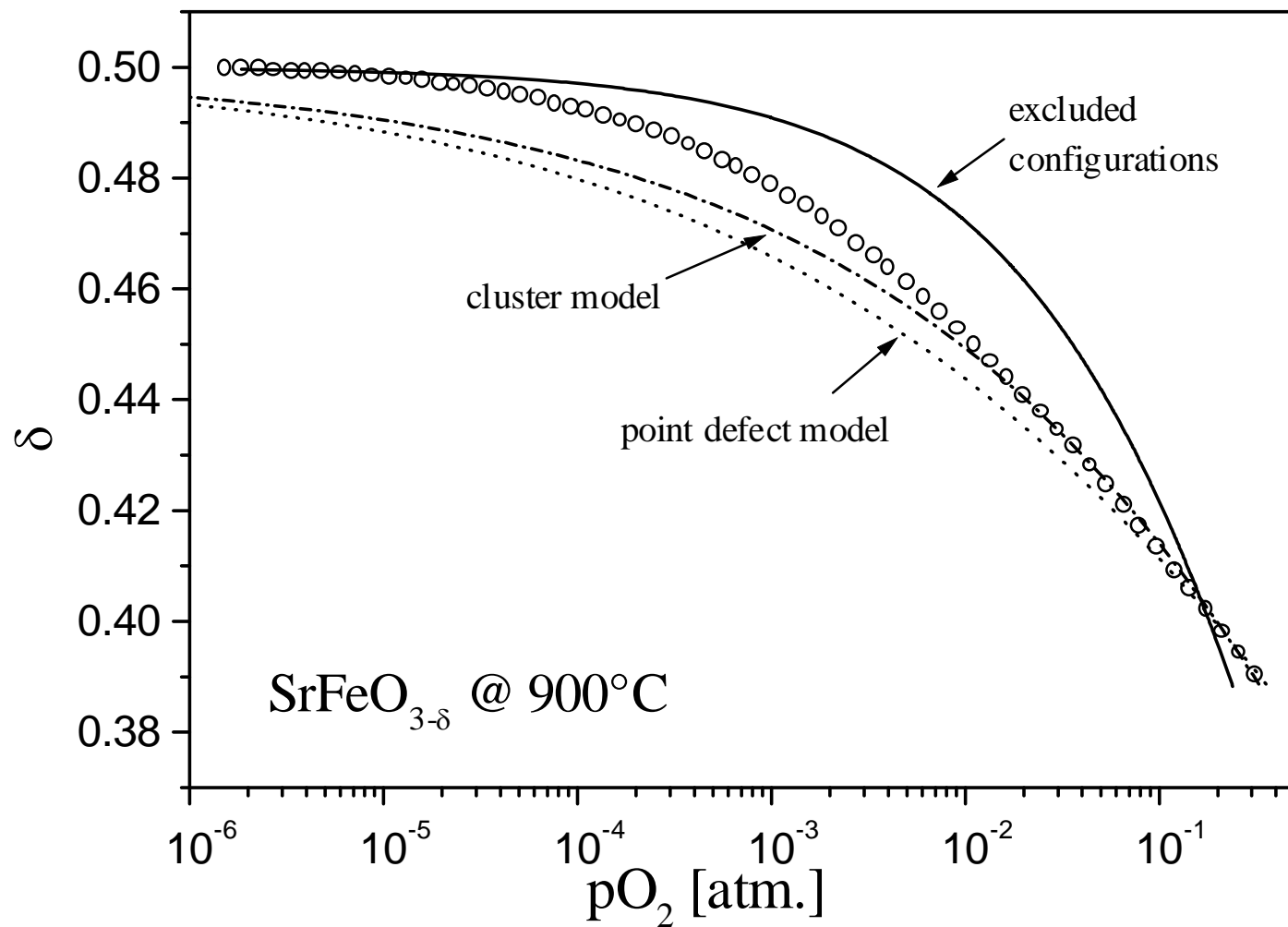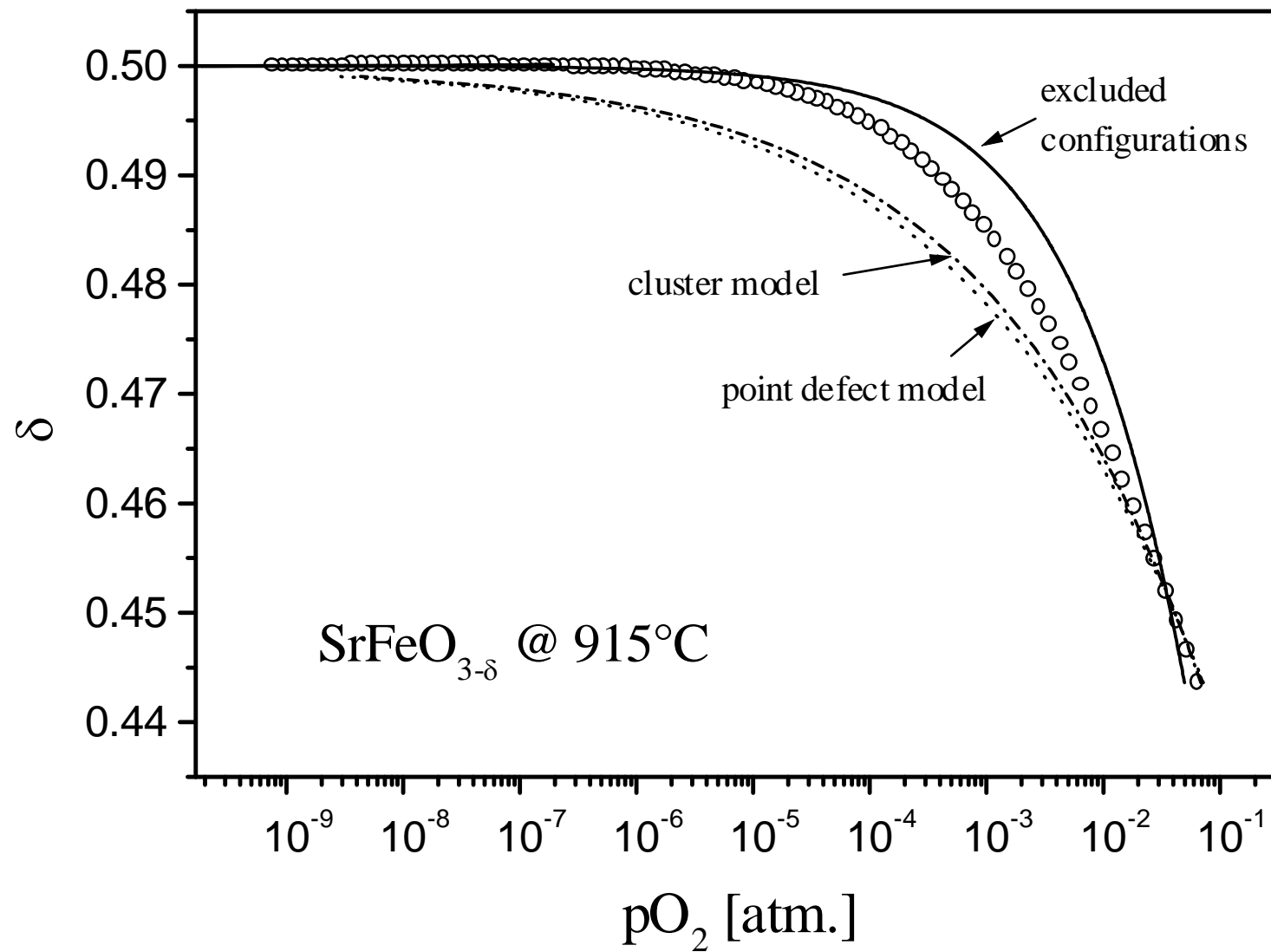
Figure 9

References

(1) Y. Teraoka, H.M. Zhang, S. Furukawa and N. Yamazoe, *Chem. Lett.,* 1985 1743.

(2) U. Balachandran, S.L. Morissette, J.J. Picciolo, J.T. Dusek, R.B. Poeppel, S. Pei, M.S. Kleefisch, R. L. Mieville, T.P. Kobylinski and C.A. Udovich, *1992 International Gas Research Conference* (Ed. H.A. Thompson), Vol. 2, p. 2499.

(3) Y. Takeda, K. Kanno, T. Takada, O. Yamamoto, M. Takano, N. Nakayama and Y. Bando, *J. Solid State Chem.*, **63**, 237 (1986); L. Fournès, Y. Potin, J.C. Grenier, G. Demazeau and M. Pouchard, *Solid State Comm.*, **62**, 239 (1987); J. Mizusaki, M. Okayasu, S. Yamauchi and K. Fueki, *J. Solid State Chem.*, **99**, 166 (1992).

(4) Y. Takeda, R. Kanno, T. Takada, O. Yamamoto, M. Takano and Y. Bando, *Z. anorg. allg. Chem.*, **540/541**, 259 (1986); J. Rodriguez, J.M. Gonzalez-Calbet, J.C. Grenier, J. Pannetier and M. Anne, *Solid State Commun.*, **62**, 231 (1987); V.V. Vashook, M.V. Zinkevich, H. Ullmann, J. Paulsen, N. Trofimenko, K. Teske, *Solid State Ionics*, **99**, 23 (1997).

(5) J. Mizusaki, M. Okayasu, S. Yamauchi and K. Fueki, *J. Solid State Chem.*, **99**, 166 (1992).

(6) L.M. Liu, T.H. Lee, L. Qiu, Y.L. Yang and A.J Jacobson, *Mater. Res. Bull.*, **31**, 29 (1996).

(7) M.T. Anderson, J.T. Vaughy and K.R. Poeppelmeier, Chem. Mater., **5**, 151 (1993).

(8) H. Kruidhof, H.J.M. Bouwmeester, R.H.E. v. Dorn and A.J. Burggraaf, *Solid State Ionics*, **63-65**, 816 (1993).

(9) A. Belzner, T.M. Gür and R.A. Huggins, *Solid State Ionics*, **40/41**, 535 (1990).

(10) A. Closset, S. Diethelm, K. Nisancioglu, J. Van herle, A.J. McEvoy, *J. Eur. Ceram.Soc.*, **19**, 843 (1999).

(11) S. Diethelm, A. Closset, K. Nisancioglu, J. Van herle, A.J. McEvoy, T.M. Gür, *J. Electrochem. Soc.*, **146**, 2606 (1999).

[12] T. Jacobsen, B. Zachau-Christiansen, K West, S. Skaarup, in: *Proc. 2nd Int. Symp. SOFC*, Athens, (Commission of the European Communities, Luxembourg, 1991) p. 795.

[13] Rita Glenne, private communication.

[14] F. W. Poulsen, G. Lauvstad and R. Tunold, *Solid State Ionics*, **72**, 47 (1994).

[15] V.V. Kharton, P.P. Zhuk, A.K. Demin, A.V. Nikolayev, A:A. Tonoyan and A.A. Vecher, *Inorg. Mater.*, **28**, 1755 (1992).

[16] W. Weppner and R.A. Huggins, *J. Electrochem. Soc.*, **124**, 1569 (1977).

[17] C. Wagner, Prog. *Solid State Chem.*, **10**, 3 (1975).

[18] F.A. Kröger and H.J. Vink, *Solid State Phys.*, **3**, 307 (1956).

[19] J.A.M. Van Roosmalen and E.H.P. Cordfunke, *J. Solid State Chem.*, **93**, 212 (1991).

[20] S. Ling, *Phys. Rev. B: Condens. Matter*, **49**, 864 (1994); S. Ling, *J. Phys. Chem. Solids*, **55**, 1445 (1994).

[21] M.H.R. Lankhorst, H.J.M. Bouwmeester and H. Verweij, *J. Am. Ceram. Soc.*, **80**, 2175 (1997).

[22] J. Van herle and A.J. McEvoy, *Ber. Bunsenges. Phys. Chem.*, **97**, 470 (1993)

[23] M.C. Kim, S.J. Park, H. Haneda, J. Tanaka, T. Mitsuhasi and S. Shirasaki, *J. Mat. Sci. Lett.* , **9**, 102 (1990).

[24] J.W. Stevenson, T.R. Armstrong, R.D. Carneim, L.R. Pederson and W.J. Weber, *J. Electrochem. Soc.*, **143**, 2722 (1996).

[25] H.J.M. Bouwmeester, H. Kruidhof and A.J. Burggraaf, *Solid State Ionics*, **72**, 185 (1994).

[26] J. Maier, *J. Am. Ceram. Soc.*, **75**, 1223 (1993).